Biophysical Chemistry 138 (2008) 83–90

Contents lists available at ScienceDirect

Biophysical Chemistry

journal homepage: http://www.elsevier.com/locate/biophyschem

Gold nanoparticles conjugated to [Tyr^3]Octreotide peptide

P.P. Surujpaul [a,b], C. Gutiérrez-Wing [a], B. Ocampo-García [a], F. de M. Ramírez [a], C. Arteaga de Murphy [c], M. Pedraza-López [c], M.A. Camacho-López [b], G. Ferro-Flores [a,*]

[a] Instituto Nacional de Investigaciones Nucleares, Carretera México-Toluca S/N., La Marquesa, Ocoyoacac, Estado de México. C.P 52750, Mexico
[b] Universidad Autónoma del Estado de México, Mexico
[c] Instituto Nacional de Ciencias Médicas y Nutrición Salvador Zubirán, Mexico

ARTICLE INFO

Article history:
Received 3 July 2008
Received in revised form 2 September 2008
Accepted 3 September 2008
Available online 14 September 2008

Keywords:
Gold nanoparticles-TOC
Neuroendocrine tumors
Gold nanoparticles-peptides

ABSTRACT

A multifunctional system of gold nanoparticles (AuNP) capped by the [Tyr^3]Octreotide (TOC) peptide was prepared and characterized by transmission electron microscopy (TEM) and UV–Vis, infrared and fluorescence spectroscopy. AuNP and AuNP-TOC fluorescence emission spectra were obtained both in solution and in murine AR42J-tumor tissues. Results suggest that AuNP were functionalized with TOC through interactions with the N-terminal amine of the phenylalanine, the amide groups and possibly with the indole group of the tryptophan residue. The fluorescence analyses in tissue revealed a recognition of the AuNP-TOC conjugate for the neuroendocrine tumor because of the lower energy position of the fluorescence resonance (692 nm) with respect to that of the AuNP in the same tumoral tissue (684 nm). The emission band observed in the near-infrared region (692 nm) opens the possibility for AuNP-TOC use in bioimaging.

1. Introduction

The octreotide peptide is a synthetic somatostatin analogue that specifically targets somatostatin receptors. Somatostatin is a cyclic peptide comprised of 14 amino acids that plays an important role in the secretion of hormones, such as insulin, glucagon and the growth hormone. Pituitary adenomas and several neuroendocrine tumours such as pancreas and lung cancer over-express somatostatin receptors [1]. Octreotide (OC) was developed for the suppression of somatostatin hypersecretion to control neuroendocrine disease symptoms. OC contains eight amino acids retaining an internal disulfide crosslink (Cys–Cys) to constrain the geometry of the four essential amino acids (Phe^3, Trp^4, Lys^5, Thr^6). The substitution of Phe^3 with Tyr^3 ([Tyr^3]OC=TOC) increases the peptide hydrophilicity thus improving the biodistribution characteristics. In 1989 Krenning *et al.* synthesized TOC to bind iodine 123 to the tyrosine residue. In spite of the limitations of this radiopharmaceutical because of *in vivo* dehalogenation, it was applied successfully in clinically imaging several types of cancer tumours [2,3]. TOC labeled with technetium-99m (^{99m}Tc-TOC) is currently used as a stable complex to detect neuroendocrine tumors by molecular imaging in nuclear medicine [4–7].

Nanoparticles can be defined as a particle of any material having dimensions of 100 nm or less with novel properties that distinguish them from bulk material due to size and surface effects [8,9]. The use of nanoparticles for any application is strongly dependent on their physicochemical characteristics and interactions with surface modifiers. Gold nanoparticles (AuNP) undergo a plasmon resonance with light incidence and are resistant to oxidation. Both properties are relevant for possible applications in optical biodetection, cellular imaging and photo-thermal therapeutic medicine [8–12].

Optical properties of AuNP have been widely studied especially the Surface Plasmon Band (SPB) observed in the UV–Vis spectra. The photoluminescence properties have been scarcely explored in spite of the fluorescence character of some AuNP as already observed in some aqueous and organic systems [13–17]. AuNP can act as an optical nanoantenna enhancing the luminescence of organic molecules [14,16–19]. Organic molecules such as those containing acetamide-like peptides can be good candidates for developing the application of AuNP as biosensors in biomedicine and bioanalytical fields [13–15].

A high selectivity for the receptor site in the target cell is necessary for the biomedical use of a targeting molecule. Specificity remains a significant practical challenge for the use of nanoparticles *in vivo*. This challenge is being addressed by the incorporation of cell-targeting peptides or antibodies on the nanoparticle surface [20–25].

A macromolecular AuNP capped by TOC could form stable and uniform multifunctional systems. Attaching multiple units of the receptor-specific peptide to one nanoparticle could be a useful tool in the imaging or therapy of tumors over-expressing somatostatin receptors. As such the AuNP-TOC conjugate may benefit from a second passive targeting behavior due to the enhanced permeability and retention (EPR) effect for macromolecular agents in solid tumors [26].

The preparation, physical, chemical and optical properties, in solution and in biological tissues, were determined in order to evaluate

* Corresponding author. Tel.: +52 55 53297200x3863; fax: +52 55 53297306.
E-mail address: gff@nuclear.inin.mx (G. Ferro-Flores).

0301-4622/$ – see front matter © 2008 Elsevier B.V. All rights reserved.
doi:10.1016/j.bpc.2008.09.005

the biomedical potential of the gold nanoparticles capped by [Tyr^3] Octreotide.

2. Experimental

2.1. Materials

The ter-butyl carbonate (Boc) protected lysine of the TOC-Boc peptide (Tyr^3, Lys (Boc)^5)–Octreotide (H–(D)–Phe–Cys–Tyr–Trp–Lys (Boc)–Thr–Cys–Thr(ol)) was synthesized by Bachem (California, USA) with purity>98% as analyzed by reversed phase high performance liquid chromatography (RP-HPLC) and mass spectroscopy. The Boc-protected lysine in the TOC peptide was used to avoid any lysine interaction with AuNP which could affect the TOC's biological activity since it is the key biological active site [1–7]. Hydrogen tetrachloroaurate trihydrate ($HAuCl_4 \cdot 3H_2O$, 99.9%), sodium citrate (99%) and all the other reagents were purchased from Sigma-Aldrich Chemical Co. and used as received.

2.2. Synthesis

Gold nanoparticles (AuNP) were synthesized by the citrate reduction method [27] at a Au: sodium citrate molar ratio of 1:1.5. Under vigorous stirring, 6.25×10^{-6} mol of $HAuCl_4$ were dissolved in 35 mL of deionized water at 75 °C, followed by the addition of the calculated amount of sodium citrate. The reaction was continued for 30 min, obtaining a stable dispersion with no noticeable precipitation.

AuNP-TOC conjugate was prepared by mixing 0.5 mL of 0.1 mM TOC-Boc with the AuNP at a molar ratio of Au:TOC-Boc 1:1. The mixture was left under continuous stirring for 30 min.

Lys-Boc deprotection was carried out by adding 0.3 mL of trifluoroacetic acid to the AuNP-TOC-Boc solution. The total volume was reduced to 1 mL under vacuum and then filtered through a 0.22 μm membrane (Millipore Co.) to remove any precipitate. The conjugate was purified by two consecutive ultracentrifugations at 14,000 g for 20 min (Sorvall Superspeed RC2-B). The supernatant was decanted and the peptide-capped gold nanoparticle pellet was resuspended in 3 mL of injectable water (Pisa®, Mexico). Two milliliters of the AuNP-TOC solution were lyophilized and 1 mL was kept in solution. Both were stored at 4 °C.

2.3. Characterization

2.3.1. TEM

The morphology and size distribution of the synthesized AuNP and of the AuNP-TOC conjugate were studied by transmission electron microscopy (TEM) in a JEOL-2010F microscope operating at 200 kV. Samples were prepared for analysis by evaporating a drop of aqueous product on a carbon-coated TEM copper grid.

2.3.2. ICP-OES

The content of gold in AuNP and AuNP-TOC solutions was determined by inductively coupled plasma optical emission spectrometry (ICP-OES, Thermo Jarrell Ash, Atomscan Advantage).

2.3.3. UV–Vis spectrophotometry

Absorption spectra in the range of 200–800 were obtained with a Unicam UV4-200 spectrometer using 1cm quartz cuvette. All reactions were followed by UV–Vis analysis to monitor the AuNP surface plasmon band at 520–531 nm. For the Au-TOC analysis, the original sample was diluted with injectable water (1:10).

2.3.4. Infrared spectroscopy

The infrared spectra of the lyophilized powder were measured on a Perkin Elmer System 2000 spectrometer with an ATR platform (Pike Technologies) by applying the Attenuated Total Reflection Fourier Transform Infrared (ATR-FTIR) spectroscopy from 500 to 4400 cm^{-1}. A finely grounded solid sample was pressed on the diamond crystal by ATR while measuring.

2.3.5. Fluorescence spectroscopy

Emission and excitation fluorescence spectra of TOC, AuNP and AuNP-TOC solutions, and tissue samples at room temperature (18 °C) were recorded on a Perkin Elmer LS-55 low resolution Luminescence spectrometer from 200 to 900 nm. Spectra were corrected using the instrumental function of the spectrometer. Using this equipment the measured intensity depends on the experimental conditions and the particular emission property of the sample. Tissue samples were analyzed as thin films (about 1 mm thick, 4 mm diameter). Samples were excited at 277 nm corresponding to the excitation of the bonded peptide and 522 nm for the AuNP with excitation and emission slits set at 9. Filters of 430 nm and 515 nm were used in recording excitation and emission fluorescence spectra to minimize Raleigh and Raman scatterings. In the case of AuNP a 290 nm filter was also used to investigate the excitation spectrum due to the citrate stabilization.

2.4. Molecular modeling

The TOC-Boc peptide molecule was built taking into account valence, bond type, charge and hybridization. The minimum energies (Molecular Mechanics calculations by Augmented MM3 procedure), the lowest energy conformer (CONFLEX procedure) and heats of formation (Quantum-mechanical calculations by MOPAC/PM5 and MOPAC/PM5/COSMO procedures) associated with the optimized geometry of its structure were calculated using the CAChe Pro 5.02 and/or 5.04 program package for windows® (Fujitsu Ltd., 2000-2001). Sequential application of Augmented MM3/CONFLEX procedures yielded the most stable conformers for the TOC-Boc structure, while MOPAC/PM5/COSMO procedures evaluated the solvent effect on TOC-Boc stabilization.

2.5. Cell lines

The AR42J murine pancreatic cancer cell line (ATTC, Rockville, MD, USA) over-express somatostatin receptors. The cells were routinely cultivated at 37 °C in 5% CO_2 and 95% humidity in Dulbecco's modified Eagle's medium supplemented with fetal-bovine-serum and added antibiotics.

2.6. Cell microscope fluorescence image

AR42J cells (1.7×10^5) were incubated with 100 μL of AuNP or AuNP-TOC colloidal solution or saline solution (control) at 37 °C for 1 h. Afterwards, treated and control cells were examined by fluorescence microscopy using excitation filters of 460–495 nm (Zeiss Axiomat, West Germany).

2.7. Animal model

Tumor uptake studies in mice were carried out according to the rules and regulations of the Official Mexican Norm 062-ZOO-1999.

Athymic male mice ($n=4$, 20–22 g) were kept in sterile cages with sterile wood-shavings beds, constant temperature, humidity, noise and 12:12 light periods. Water and feed (standard PMI 5001 feed) were given *ad libitum*.

AR42J tumors were induced by subcutaneous injection of AR42J cells (1×10^6) resuspended in 0.2 mL of phosphate-buffered saline, into the upper back of 6–7 week old nude mice. The injection sites were observed at regular intervals for the appearance of tumor formation and progression. AuNP (0.05 mL, 55 mg/L of Au) or AuNP-TOC conjugate (0.05 mL, 0.05 mg/L of Au) was injected in the tail vein.

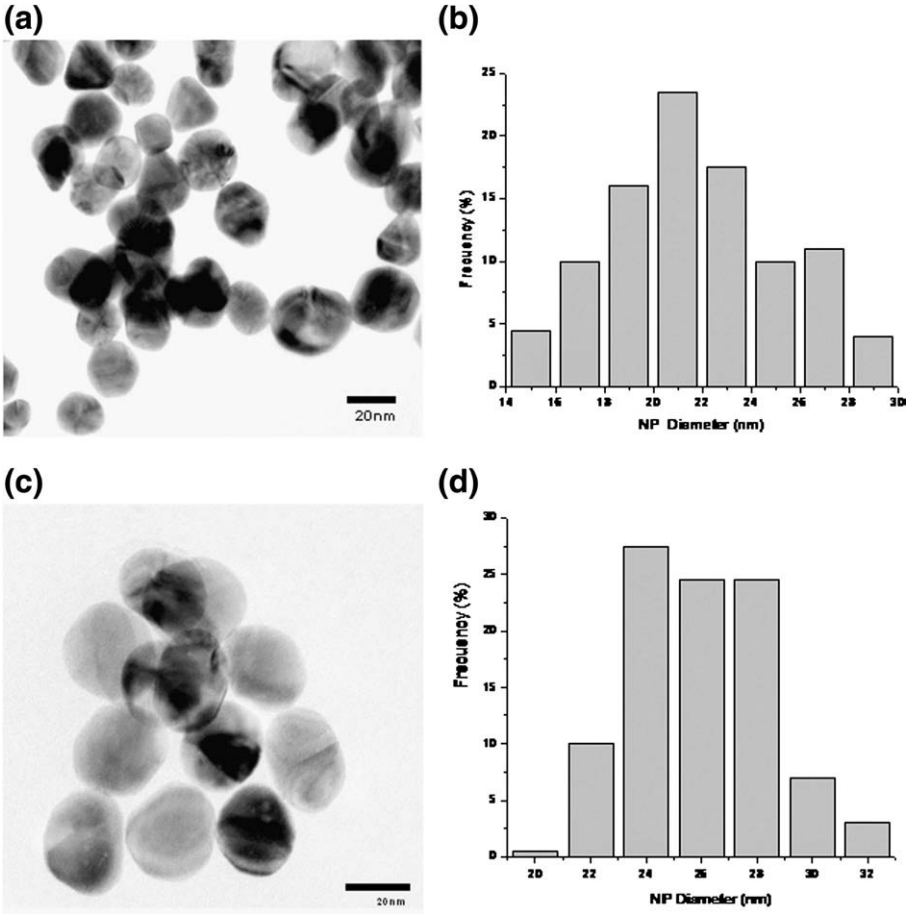

Fig. 1. (a) TEM image of AuNP, (b) size distribution of AuNP, (c) TEM image of AuNP-TOC, (d) size distribution of AuNP-TOC.

The mice were sacrificed at 2 h post-injection. Kidneys (excretory organ) and tumor samples were dissected for fluorescence analysis.

3. Results

The AuNP prepared were stable showing no visible coalescence. Particle size distribution ranged from 14 to 30 nm with a mean diameter of 21 ± 3.8 nm as determined by TEM analysis (Fig. 1a,b). Most of the particles showed structures with a spherical tendency, however, other shapes such as hexagons, triangles and rhombohedra were also observed. The average particle size of the AuNP-TOC conjugate was shifted to higher values due to some aggregation among particles and their interactions with the peptide. This behavior was previously reported with other capping biomolecules such as cysteine [28]. In this case, size distribution is centered at 26 nm and extends from 15 to 35 nm and a SD of 3.5 (Fig. 1c,d).

3.1. Spectroscopic characterization

3.1.1. UV–Vis spectrophotometry

The absorption peak wavelengths for TOC-Boc, AuNP and AuNP-TOC are shown in Table 1. The red colloidal AuNP dispersion (21 nm) shows only one wide characteristic absorption band [9] centered at 531 nm.

The peptide TOC-Boc showed an absorption spectrum with maximum of 278 nm, defined shoulder at 289 nm and less-defined shoulder at 273 nm pertaining to the electronic transition of the phenyl groups of the tryptophan residue (278 and 289 nm) and tyrosine (273 nm).

A low intensity plasmon resonance band centered at 558 nm was detected even when the AuNP-TOC was present in a low concentration (0.05 mg/L Au) with respect to the initial reaction mixture (55 mg/mL) due to the purification process as determined by ICP-OES.

3.1.2. Infrared spectroscopy

The main bands and the assignation of the ATR-FTIR TOC-Boc, AuNP and AuNP-TOC spectra of the lyophilized samples are shown in Table 2. These spectra were smoothed and normalized in order to define the most important bands. Fig. 2 shows the AuNP, TOC-Boc and AuNP-TOC spectra.

3.1.3. Fluorescence spectroscopy

The TOC-Boc, AuNP and AuNP-TOC excitation spectra and AuNP-TOC emission spectra in fluorescence mode are shown in Fig. 3. Fig. 3a reveals a simple excitation spectrum for AuNP and more structured ones for AuNP-TOC. The excitation spectra of the AuNP reveals one band centered at 283 nm which corresponds to the $n \rightarrow \pi^*$ transition of the carbonyl groups of the citrate capping the AuNP. This transition of carbonyl is observed at approximately 300 nm in the absorption spectra of pure organic compounds [31].

Table 1
UV–Vis absorbance bands (nm) obtained for TOC-Boc, AuNP and AuNP-TOC

Characteristic	TOC-Boc	AuNPs	AuNP-TOC
Maximum	278	531	558
Description	Asymmetric at 278	Intense asymmetric peak	Weakly intense peak
Maximum peak interval	246 to 304	434 to 612	556 to 560
Shoulders	273, 289	261, 366	290

Table 2
Main IR vibration frequencies (cm^{-1}) for TOC-Boc, AuNP and AuNP-TOC in the solid state obtained by ATR-FTIR spectroscopy

Functional Group (vibrations)	TOC-Boc	AuNP	AuNP-TOC
secondary amides (N–H stretch)	3279_s, 3073_{ms}		$3100–3500_s$; Centered at 3311
NH_2-lysine (N–H stretch) - TOC			$3800–3600_m$
Moisture	$3800–3600_w$	$3800–3600_w$	
carboxylic acid (H–O-stretch)		(2980–2830) 2921_w	
$–CH_2$, CH_3; –CH (asym stretch)	2931_m,2808_m, 2708_{sh},2604_{sh}		2914_s; 2721_m
CH_3, CH_2: H–C-deformation	1437_{sh},		
–CH-out of plane deformation: aryls, disubstituted rings, CH_2 rocking	$832–650_{ms}$		
$–CH_2–$		948_m, 786_m 647_m	
Amide I, (C═O stretching)	1648_{vs},		1657_{mw},
Amide II ((N–H bending mostly))	1528_{vs}		
C–O-stretch	1160_s, 1086_{sh}		1023_{vs},
═CH–N- (indole ring bend)	994_m, 943_{sh}		868_{mw}
HO-alcohol of side chains (bend	$1419_{m,sh}$, 1383_m 1356_m, 1249_{ms}		1417_m, 1307_w, 1248_{mw}
H–O phenol of tyrosine (bend)			
$–C–CH_2–OH$ of citric acid		1068_{ms}	
carboxylic acid (H–O-stretch)		2918_{mw},1945_{mw}, 1856	$2000–1730_w$
Carboxylic; CO_2^- (sym and asym)		1714_{vs} ; 1563_{sh}, 1540_{sh} and 1396_m, 1325_{mw}, 1204_w	

vs: very strong; s: strong; ms: medium strong; m: medium; mw: medium weak; w: weak; s: shoulder.

The emission spectrum of AuNP-TOC using a 515 nm filter is weaker but well-defined compared to using the 430 nm filter (Fig. 3b). The intensity relation of the 436 nm band (430 nm filter, I=9.03) due to the peptide with the net emission of the 523 nm band (515 nm filter I=2.07) due to the AuNP in the AuNP-TOC is approximately 3:1 (Fig. 3b). Under the same experimental conditions, the latter emission is not seen in AuNP-citrate spectrum but instead a very weak structured spectrum with no identifiable maximum is seen (Table 3), demonstrating that fluorescence energy transfer from TOC to the AuNP occurs. However, the energy transfer does not occur completely since the peptide emission band is still present. A typical FRET cannot be affirmed because the conjugated peptide band (donor) is red shifted with respect to the free peptide which confirms a certain covalent character in the AuNP-TOC interactions. This suggests that AuNP-TOC distances are shorter than the typical Förster distance for FRET (R_o=1–100 nm).

Table 3 shows the main emission bands and the shoulders of the TOC-Boc, AuNP, AuNP-TOC, AuNP tissue and AuNP-TOC in tissues and their emission spectra recorded under exactly the same experimental conditions are shown in Fig. 4. The TOC-Boc in water has an emission spectrum with an intense band centered at 422 nm (Fig. 4a).

AuNP was excited with λ_{exc}=277 nm (Fig. 4d) (nearly corresponding to maximum citric absorbance) and with λ_{exc}=522 nm (maximum AuNP absorbance) in order to find out the extent of the fluorescence emission of the citrate-capped AuNP. The excitation at 277 nm yielded a spectrum centered at 429 nm with shoulders at 550 and 620 nm (Table 3).

The emission spectrum for the AuNP-TOC conjugate reveals that the peptide is bonded to the nanoparticle since the emission band of the free TOC-Boc (422 nm) is shifted 761 cm^{-1} to lower energy (436 nm) and widened in the region from 394 to 710 nm, which indicates the AuNP emission (Fig. 4b). The spectrum 4C of AuNP-tumor is structured with shoulders in the same regions as the AuNP spectrum (Fig. 4d).

3.1.4. Tumor uptake fluorescence

Before studying the excitation and emission spectra of the AuNP and of the AuNP-TOC conjugate in tissue, the emission spectrum of a control tissue (kidney) without any treatment was obtained. The emission bands observed with λ_{exc}=277 nm corresponded to substances present in blood and tissue (e.g. porphyrin at 442 nm) and were different from those observed as characteristic of AuNP or AuNP-TOC in tissue (Table 3). The emission band assigned to the TOC-component in the AuNP-TOC-Tumor revealed a maximum emission at 430 nm (λ_{exc}=277 nm), demonstrating a shift to a higher energy with respect to the AuNP-TOC in solution (436 nm). This suggests that the TOC conjugated to the AuNP presents a tumor biological recognition since the formation of the TOC-Receptor is entropically unfavorable [29].

It is important to compare two prominent results observed in the AuNP-TOC-Tumor emission spectra and in the AuNP-tumor at 522 nm excitation wavelength, 1) the AuNP-tumor presents a defined band at 684 nm and the AuNP-TOC-Tumor at 692 nm (Fig. 5), 2) their intensity ratio is: I_{684nm}/I_{692nm}=10/1.25=4 while their concentration ratio is [Au (AuNP)]/[Au (AuNP-TOC)]≥1000.

3.1.5. Kidney with AuNP-TOC

These spectra were obtained with the purpose of identifying a possible *in vivo* rupture of the AuNP-TOC binding. In the kidney-AuNP-TOC spectrum with λ_{exc}=277 nm, the emission band at 436 nm corresponded exactly to the AuNP-TOC band in solution and therefore to the conjugate without biological interaction. With a wavelength

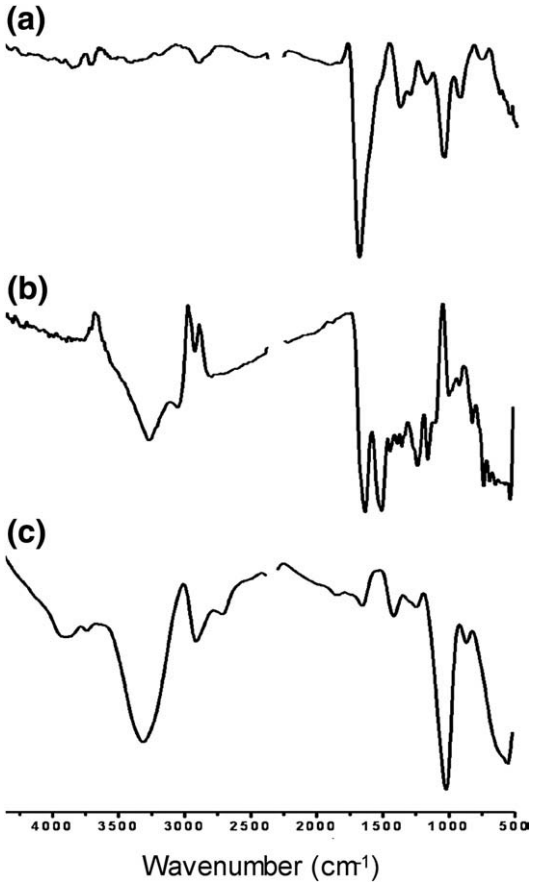

Fig. 2. ATR-FTIR spectra of the powdered lyophilized samples of a) AuNP, b) TOC-Boc and c) AuNP-TOC, at room temperature.

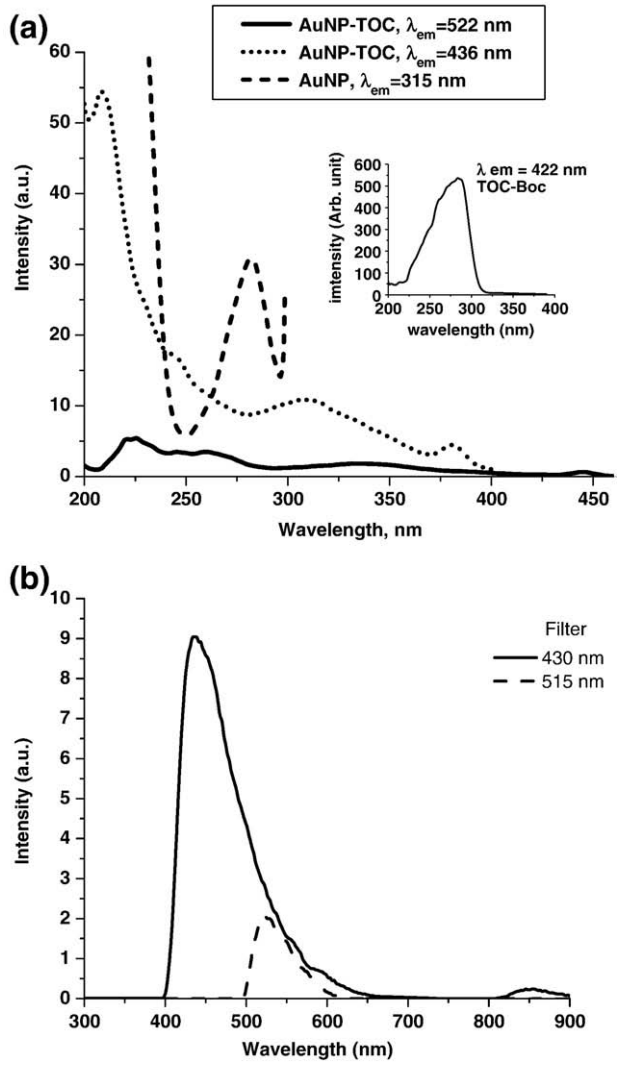

Fig. 3. a) Excitation fluorescence spectrum of AuNP-TOC, AuNP and TOC-Boc (inset). Excitation and emission slits: 9 nm b) Emission fluorescence spectrum of AuNP-TOC: λ_{exc}=277 nm, excitation and emission slits: 9 nm, using two filters.

excitation at 277 nm and a 515 nm filter the band pertaining to the AuNP in the conjugate was observed at 531 nm and close to the band of the AuNP-TOC in solution (528 nm) suggesting no biological interaction.

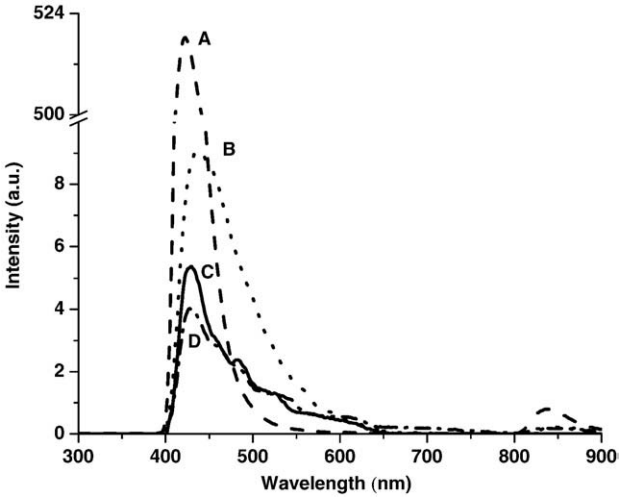

Fig. 4. Emission fluorescence spectrum for A) TOC-Boc (in solution), B) AuNP-TOC (in solution), C) AuNP-TOC (in tumor) and D) AuNP (in solution). λ_{exc}=277 nm, excitation and emission slits: 9 nm; filter=430 nm.

3.1.6. Cell fluorescence

After incubation of AR42J cells with AuNP-TOC, AuNP and saline (control), a more intense fluorescence in AuNP-TOC treated cells was qualitatively observed (Fig. 6). This is indicative of a higher uptake of AuNP-TOC respect to the AuNP in cancer cells because of the specific somatostatin receptor recognition.

3.1.7. Molecular modeling

The final energy of the most stable optimum structure of the macrocyclic peptide TOC-Boc was 130 kcal/mol (Augm MM3). The important energy parameters that contribute to the optimized structure's final energy are the hydrogen bond and the Van der Waals energies. The heat formation calculation (E=−542 kcal/mol) of the molecule in the absence of water yielded a structure in which intramolecular hydrogen bonding was not observed, leading then to molecules with intermolecular hydrogen bonds. This maintains a narrow relation with the peptide mobility as demonstrated by the 151 stable conformers calculated by CONFLEX, where the energy of the most stable one is 106 kcal/mol. The presence of water promotes molecule stability (E=−602 kcal/mol) with simultaneous breaking of any intermolecular bond formed, leaving it free to react. The optimum conformer TOC-Boc structure is shown in Fig. 7.

The average calculated cavity diameter of the asymmetric cyclic peptide structure using the resultant structure of MOPAC/PM5/COSMO

Table 3
Fluorescence emission bands (nm) of the TOC-Boc, AuNP, AuNP-TOC, AuNP-TOC-Tumor and AuNP-TOC-Kidney

$\lambda_{excitation}$	Emission filter	TOC-Boc	AuNP	AuNP-TOC	AuNP-tumor	AuNP-TOC-tumor	AuNP-TOC-kidney
277 nm	430	Maximum 422 (spectrum not structured)	Maximum 429	Maximum 436 (structured spectrum: 523, 538, 557, 568, 596, 603, 609, 621)	–	Maximum 430	Maximum 436
			Shoulders: 550, 620			Shoulder 482 (structured spectrum 460, 486, 525, 560, 599, 627)	
	515	–	Weak structured spectrum: maximum not detectable	Maximum 523,528 (structured spectrum: 540, 550, 575, 595, 602, 604, 610, 616, 621)	Maximum 529 (structured spectrum 598, 675, 760, 824)	–	Maximum 531
522 nm	430	–	676	*not detectable	–	–	–
	515	–	Weak structured spectrum: maximum not detectable	*not detectable	Peak at 684	Shifted to 692 respect to the AuNP-Tumor peak	Maximum 592
							Shoulder 541

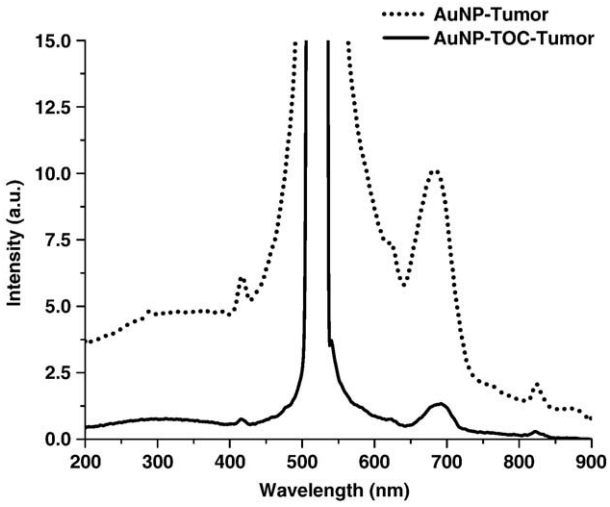

Fig. 5. Emission fluorescence spectrum for AuNP and AuNP-TOC in the murine AR42J-tumor tissue. λ_{exc}=522 nm, excitation and emission slits: 9 nm; filter=515 nm.

was of 6.7±1.4 Å. As a result, any substance with a size range beyond this interval would not be able to fit in its cyclic cavity. In this structure, the bond angles and bond distances are C21–C23–S26 (111.47°, 1.821 Å); C113–C115–S118 (111.01°, 1.796 Å); C23–S26–S118 (102.69°), C115–S118–S26 (106.94°). The dihedral and improper torsion angles are C23–S26–S118–C115 (dih −106.54°; imptor 41.35°) C115–S118–S26–C23 (dih −106.54°; imptor 39.06°). The S–S distance of 2.055 Å confirms that the cyclic peptide is moderately constrained and that the S–S bond is stable. Nevertheless, these disulphide bonds, amino acid side chains as well as the primary amine of phenylalanine and the amide groups outside the macrocyclic peptide structure remain free and exposed to the medium (Fig. 7b).

4. Discussion

According to the molecular modeling, the size of TOC-Boc-macrocyclic peptide would prevent the inclusion of nanometric-sized substances. However, its conformational arrangement leaves the functional groups of its side-chains exposed to the medium. This permits the interaction of the peptide molecules with the nanoparticle and once positioned with their free functional groups they could form cavities through intermolecular hydrogen bonding, where nanometric-sized species can be included and stabilized in a similar way to what occurs with the dendrimers [8,22]. The high negative heat formation obtained in the presence of water (MOPAC/PM5/COSMO) confirms that the cyclic molecule of TOC-Boc is stable in water (the internal disulphide crosslink is retained) and that its interaction with the AuNP is through the N-terminal amine, amides and indole groups outside of the macrocyclic structure. However, the high mobility of this macrocycle (151 calculated conformers) opens the possibility of the interaction of the disulphide bridge with the nanoparticle. According to the molecular modeling, if TOC were not Boc protected in the position Lys(Boc)[5], the main interaction with the AuNP would be through the primary amine of lysine (key site in TOC for the biological recognition) of such other reported peptides [22,24].

Their stereochemical arrangement constrained by the peptide ring seems to play the most important role in the functionalization of AuNP which was revealed in the infrared spectrum of AuNP-TOC. The changes observed in the infrared spectrum of AuNP-TOC with respect to those of the AuNP and of TOC-Boc such as broadening of the H–N bands, reduction in the intensity of some of them or increase in others have been also mentioned [22,24,25,30–32]. In TOC-Boc, the CH vibrations of the phenylalanine and tryptophan aryl appear at 832–650 cm^{-1} [23] and disappear in the AuNP-TOC. This suggests that the N-terminal amine group separated from the aryl by methylene groups in the Phe is involved in the AuNP bond. A possible indole (tryptophan side chain) AuNP interaction is proposed since the bands assigned to the indole ring deformation are not observed; instead a less intense band at lower energy also appears due to the indole bending modes (Table 2).

The amide II vibrations due to H–N bending are no longer seen in the AuNP-TOC spectrum and that of amide I from –C=O stretching is weakened and shifted to a higher energy. The vibration from the N-terminal amine group is masked by the amide regions. Moreover, the band at 1160 cm^{-1} corresponding to C–O stretching of C=C–OH from tyrosine and alcohol of threonines in the TOC-Boc is seen as a broad intense band centered at 1023 cm^{-1}. This means that OH from alcohol derivatives do not interact with AuNP but reflects the symmetry change of the peptide caused by the AuNP-TOC interaction.

From the IR spectra it is also clear that the TOC displaces the carboxylic groups of the citric acid and significantly interacts with the AuNP (Table 2 and Fig. 2).

Formal studies on the luminescence from AuNP in aqueous media are not commonly reported [13–16]. In this work, the characteristics of the excitation and emission spectra of AuNP-TOC suggest a significant interaction of TOC with AuNP. The TOC-Boc emission (422 nm) is due to its phenyl rings but the AuNP-TOC is red-shifted (436 nm) caused

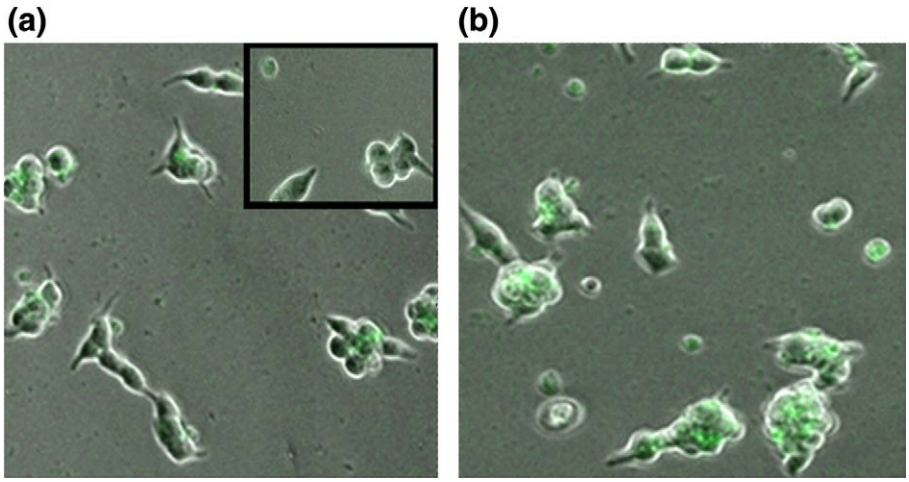

Fig. 6. Fluorescence microscopy images of AR42J cells incubated with (a) AuNP and (b) AuNP-TOC. Inset: AR42J with saline (control). Observe qualitatively a more intense fluorescence in AuNP-TOC treated cells.

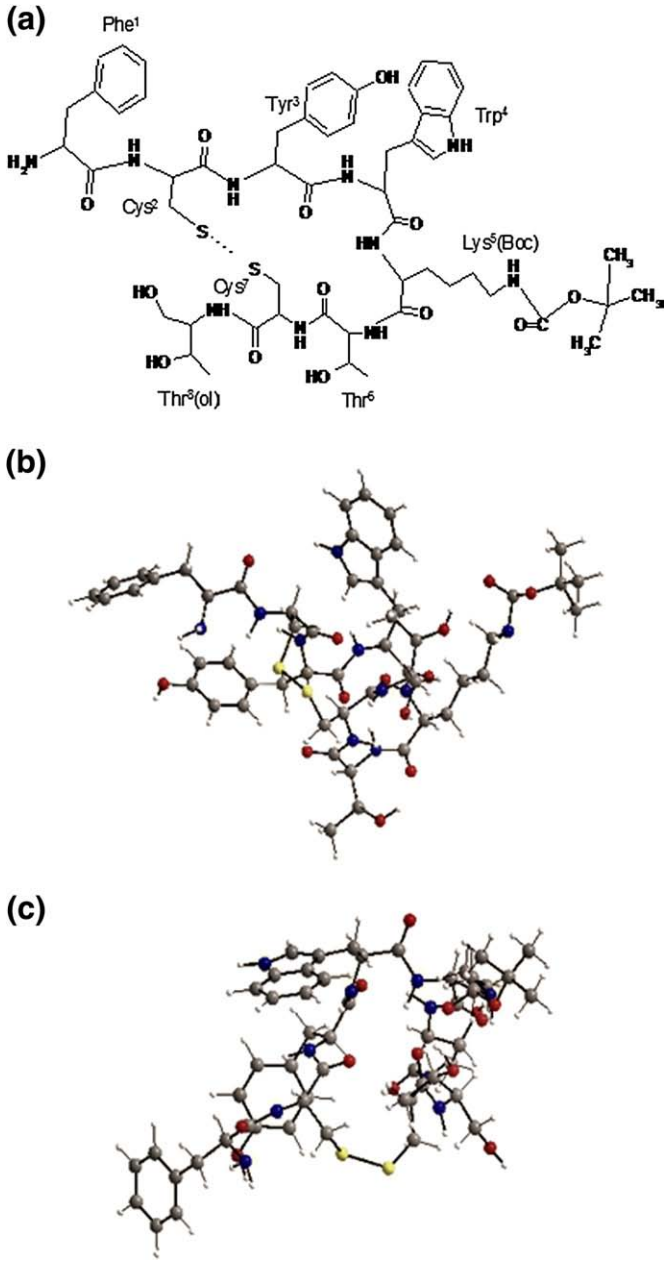

Fig. 7. (a) TOC-Boc sketch (b) Structure of TOC-Boc calculated by Molecular and Quantum Mechanics (E=106 kcal/mol) (c) Other view of the modeled structure. Note the cyclic cavity with size 0.67±0.14 nm.

by the primary amine (Phe) and amide interactions with the AuNP. It is known that the nanoparticle size and its functionalization degree define the plasmon energy band [15], which is an indication of the interaction force of AuNP-peptide. In fact, it has been demonstrated that the particle plasmon resonance maintains an intrinsic relationship with the excitation and emission fluorescence of this type of material [9,16]. In the AuNP, AuNP-TOC, AuNP-tumor, and AuNP-TOC-tumor spectra (Figs. 4 and 5), the size interval and the geometrical forms (spherical, hexagonal, and triangular) of nanoparticles along with the conformational properties of the peptide seem to be responsible for the multiple peaks in the interval 500 nm to 750 nm and indicates the presence of the AuNP.

It is important to mention that the samples used for this study were very dilute solutions, for which, it was necessary to use wide slits and filters. The 515 nm filter was used to minimize the water Raman and Rayleigh scattering, the scattered excitation light, the harmonic due to water emission spectrum and intrinsic emissions. In the case of the tissue samples the intrinsic emission due to blood components such as porphyrins (λ_{exc}=442 nm) and the excitation scattered light were still present since they were not completely eliminated (Fig. 5).

In general, the tissue fluorescence analyses suggest a AuNP-TOC conjugate recognition for the neuroendocrine tumor because of the lower energy position of the emission band (692 nm) with respect to that of the AuNP in the same tumoral tissue (684 nm). The luminescence energy transfer from TOC to AuNP is also manifested in its interaction with the tissue since the intensity ratio AuNP/functionalized AuNP was lower than 5 but the concentration ratio was a factor of 1000 higher. It is evident that although the gold nanoparticles can interact with the tumor, they significantly improve their capacity to be recognized by the protein receptor upon being functionalized with TOC.

The fundamental barriers to optical imaging of tissue are high light scattering, intrinsic fluorescence and high absorption by hemoglobin in the mid-visible band. Near-infrared light of 650 to 900 nm achieves the highest tissue penetration due to minimal absorbency of the surface tissue [10], therefore the AuNP-TOC-Tumor emission band at 692 nm observed in the fluorescence spectrum opens the possibility for AuNP-TOC use in bioimaging.

5. Conclusions

In spite of the fact that the purified AuNP-TOC conjugate resulted to be very diluted and that the size interval of the AuNP is extensive, the characteristics of the absorption spectra, the vibration frequencies displacement and the fluorescence emission shifts indicate that the gold nanoparticles were functionalized with the [Tyr^3]Octreotide peptide through interactions of covalent character with the N-terminal amine of the phenylalanine and amide groups. The AuNP-TOC spectra also suggest interactions of the AuNP with the TOC tryptophan residue.

The emission shifts indicate that the AuNP-TOC conjugate is recognized by the neuroendocrine tumor in a more selective manner than the AuNP. Although AuNP interact with the tumor, their conjugation with TOC improves their capacity to be recognized by the protein receptor and enhances their fluorescence properties.

Acknowledgments

This work was partially supported by the National Council of Science and Technology (CONACYT-MEXICO J49603) and the International Atomic Energy Agency (IAEA RC14539).

References

[1] J.C. Reubi, Peptide receptors as molecular targets for cancer diagnosis and therapy, Endocr. Rev. 24 (2003) 389–427.
[2] E.P. Krenning, W.A.P. Breeman, P.M. Kooij, J.S. Lameris, W.H. Bakker, J.W. Koper, L. Ausema, J.C. Reubi, S.W.J. Lamberts, Localisation of endocrine-related tumours with radioiodinated analogue of somatostatin, Lancet 1 (1989) 242–244.
[3] E.P. Krenning, D.J. Kwekkeboom, W.H. Bakker, W.A.P. Breeman, P.M. Kooij, H.Y. Oei, M. van Hagen, P.T. Postema, M. de Jong, T.J. Visser, A.E.M. Reijs, L.J. Hofland, J.W. Koper, S.W.J. Lamberts, Somatostatin receptor scintigraphy with [^{111}In-DTPA-D-Phe^1]- and [^{123}I-Tyr^3]-octreotide: the Rotterdam experience with more than 1000 patients, Eur. J. Nucl. Med. 20 (1993) 716–731.
[4] M. Gabriel, C. Decristoforo, E. Donnemiller, H. Ulmer, W. Rychlinski, S.J. Mather, R. Moncayo, An intrapatient comparison of ^{99m}Tc-EDDA/HYNIC-TOC with ^{111}In-DTPA-octreotide for diagnosis of somatostatin receptor-expressing tumors, J. Nucl. Med. 44 (2003) 708–716.
[5] A. Plachcinska, R. Mikolajczak, H.R. Maecke, A. Michalski, K. Rzeszutek, J. Kozak, J. Kusmierek, ^{99m}Tc-EDDA/HYNIC-TOC scintigraphy in the differential diagnosis of solitary pulmonary nodules, Eur. J. Nucl. Med. Mol. Imaging 31 (2004) 1005–1010.
[6] A. Gonzalez-Vazquez, G. Ferro-Flores, C. Arteaga de Murphy, Z. Gutierrez-Garcia, Biokinetics and dosimetry in patients of ^{99m}Tc-EDDA/HYNIC-Tyr^3-octreotide prepared from lyophilized kits, Appl. Radiat. Isotopes 64 (2006) 792–797.
[7] R. Czepczynski, M.G. Parisella, J. Kosowicz, R. Mikolajczak, K. Ziemnicka, M. Gryczynska, J. Sowinski, A. Signore, Somatostain receptor scintigraphy using ^{99m}Tc-EDDA/HYNIC-TOC in patients with medullary thyroid carcinoma, Eur. J. Nucl. Med. Mol. Imaging 34 (2007) 1635–1645.
[8] C. Daniel, D. Astruc, Gold nanoparticles: assembly, supramolecular chemistry, quantum-size-related properties, and applications toward biology, catalysis and nanotechnology, Chem. Rev. 104 (2004) 293–346.

[9] C. Burda, X. Chen, R. Narayanan, M.A. El-Sayed, Chemistry and properties of nanocrystals of different shapes, Chem. Rev. 105 (2005) 1025–1102.
[10] P. Sharma, S. Brown, G. Walte, S. Santra, B. Moudgil, Nanoparticles for bioimaging, Adv. Colloid Interface Sci. 123–126 (2006) 471–485.
[11] J. Chen, F. Saeki, B.J. Wiley, H. Cang, M.J. Cobb, Z.Y. Li, L. Au, H. Zhang, M.B. Kimmey, X. Li, Y. Xia, Gold nanocages: bioconjugation and their potential use as optical imaging contrast agents, Nano Lett. 5 (2005) 473–477.
[12] D. Pissuwan, S.M. Valenzuela, M.B. Cortie, Therapeutic possibilities of plasmonically heated gold nanoparticles, Trends Biotechnol. 24 (2006) 62–67.
[13] R. Elghanian, J.J. Storhoff, R.C. Mucic, R.L. Letsinger, C.A. Mirkin, Selective colorimetric detection of polynucleotides based on the distance-dependent optical properties of gold nanoparticles, Science 277 (1997) 1078–1081.
[14] X.C. Shen, L.F. Jiang, H. Liang, X. Lu, L.J. Zhang, X.Y. Liu, Determination of 6-mercaptopurine based on the fluorescence enhancement of Au nanoparticles, Talanta 69 (2006) 456–462.
[15] L. Huang, M. Zhai, J. Peng, L. Xu, J. Li, G. Wei, Synthesis, size control and fluorescence studies of gold nanoparticles in carboxymethylated chitosan aqueous solutions, J. Colloid Interface Sci. 316 (2007) 398–404.
[16] S. Kühn, U. Häkanson, L. Rogobete, V. Sandoghdar, Enhancement of single-molecule fluorescence using a gold nanoparticle as an optical nanoantenna, Phys. Rev. Lett. 97 (2006) 017402.
[17] T. Wang, D. Zhang, W. Xu, J. Yang, R. Han, D. Zhu, Preparation, characterization and photophysical properties of alkanethiols with pyrene units-capped gold nanoparticles: unusual fluorescence enhancement for the aged solutions of these gold nanoparticles, Langmuir 18 (2002) 1840–1848.
[18] J. Zhang, J.R. Lakowicz, Metal-enhanced fluorescence of an organic fluorophore using gold particles, Opt. Express 15 (2007) 2598–2606.
[19] M.F. Garcia-Parajo, Optical antennas focus in on biology, Nat. Photonics 2 (2008) 201–203.
[20] Y. Liu, M.K. Shipton, J. Ryan, E.D. Kaufman, S. Franzen, D.L. Feldheim, Synthesis, stability and cellular internalization of gold nanoparticles containing mixed peptide-poly(ethylene glycol) monolayers, Anal. Chem. 79 (2007) 2221–2229.
[21] K. Sokolov, M. Follen, J. Aaron, I. Pavlona, A. Malpica, R. Lotan, R. Richards-Kortum, Real-time vital optical imaging of precancer using anti-epidermal growth factor receptor antibodies conjugated to gold nanoparticles, Cancer Res. 63 (2003) 1999–2004.
[22] F. Porta, G. Speranza, Z. Krpetic, V.D. Santo, P. Francescato, G. Scari, Gold nanoparticles capped by peptides, Mater. Sci. Eng., B 140 (2007) 187–194.
[23] L. Burt, C. Gutierrez-Wing, M. Miki-Yoshida, M. Jose-Yacaman, Noble-metal nanoparticles directly conjugated to globular proteins, Langmuir 26 (2004) 11778–11783.
[24] R. Levy, N.T.K. Thanh, R.C. Doty, I. Hussain, R.J. Nichols, D.J. Schiffrin, M. Brust, D.G. Ferning, Rational and combinatorial design of peptide capping ligands for gold nanoparticles, J. Am. Chem. Soc. 126 (2004) 10076–10084.
[25] L. Fabris, S. Antonello, L. Armelao, R.L. Donkers, Gold nanoclusters protected by conformationally constrained peptides, J. Am. Chem. Soc. 128 (2005) 326–336.
[26] A. Maeda, J. Wu, T. Sawa, Y. Matsumura, K. Hori, Tumor vascular permeability and the EPR effect in macromolecular therapeutics: a review, J. Control. Release 65 (2000) 271–284.
[27] J. Turkevitch, P.C. Stevenson, J. Hillier, Nucleation and growth process in the synthesis of colloidal gold, Discuss. Faraday Soc. 11 (1951) 55–75.
[28] S. Aryal, B. Remant, N. Dharmaraj, N. Bhattarai, C.H. Kim, H.Y. Kim, Spectroscopic identification of S–Au interaction in cysteine capped gold nanoparticles, Spectrochim. Acta, Part A 63 (2006) 160–163.
[29] R.B. Silverman, the organic chemistry of drug design and drug action, Elsevier Academic Press, UK, 2004.
[30] D.V. Leff, L. Brandt, J.R. Heat, Synthesis and characterization of hydrophobic, organically-soluble gold nanocrystals functionalized with primary amines, Lagmuir 12 (1996) 4723–4730.
[31] S.Y. Lin, Y.T. Tsai, C.C. Chen, C.M. Lin, C. Chen, Two-step functionalization of neutral and positively charged thiols onto citrate-stabilized Au nanoparticles, J. Phys. Chem., B 108 (2004) 2134–2139.
[32] D.H. Williams, I. Fleming, Spectroscopic methods in organic chemistry, McGRAW-HILL Book Company, UK, 1980.